Author(s): Wanakai, Indire Sammy; Kareru, Gachoki Patrick; Sujee, Makhanu David; Madivoli, Shigwenya Edwin; Gachui, Maina Ernest; Kairigo, Kinoti Pius

Title: Kinetics of Rifampicin Antibiotic Degradation Using Green Synthesized Iron Oxide Nanoparticles

Year: 2023

Version: Accepted version (Final draft)

Please cite the original version:

Wanakai, I. S., Kareru, G. P., Sujee, M. D., Madivoli, S. E., Gachui, M. E., & Kairigo, K. P. (2023). Kinetics of Rifampicin Antibiotic Degradation Using Green Synthesized Iron Oxide Nanoparticles. Chemistry Africa, 6, 967-981. https://doi.org/10.1007/s42250-022-00543-w

Kinetics of Rifampicin Degradation using Green Synthesized Iron Oxide Nanoparticles

Wanakai Sammy Indire [1*], Kareru Patrick Gachoki[1]., Makhanu David Sujee[2], Madivoli Edwin Shigwenya[1], Maina Ernest Gachui[1,] and Kairigo Pius Kinoti[1,3]

[1]Chemistry Department, Jomo Kenyatta University of Agriculture and Technology, P.O Box 62,000-00200, Nairobi, Kenya

[2]School of Pure & Applied Sciences Karatina University, P.O. Box 1957-10101 Karatina, Kenya.

[3]Department of Biological and Environmental Science, University of Jyväskylä, P.O. Box 35, FI-40014 Jyväskylä, Finland

[*]Corresponding Author: wanakaisammy@gmail.com

Abstract

Presence of antibiotics in water is persistent, bio accumulative and harmful to humans and aquatic habitats hence the need to find ways of their removal. This study investigated the catalytic degradation of rifampicin using iron oxide nanoparticles synthesized using aqueous extracts of *Galinsoga parviflora*, *Conyza bonariensis* and *Bidens pilosa*. The effect of temperature, pH, time, and adsorbent dose on the rate of degradation were evaluated by carrying out the reaction in different reaction conditions. From the results obtained in this study, the percent degradation was found to be dependent on the pH, temperature, and the amount of the nanoparticles used during the study. Higher degradation efficiencies were obtained when the degradation was studied in acidic media as compared to basic and neutral media and when the temperature and the amount of the nanoparticles used were 60 °C and 20 mg, respectively. The degradation of rifampicin using iron oxide nanoparticles was found to be pseudo second order, endothermic and dependent on the reactants used during the study and variation of reaction conditions led to an increase in the percent degradation observed. In conclusion, iron nanoparticles synthesized using *Galinnsoga parviflora*, *Conyza bonariensis* and *Bidens pilosa* could be used catalytically in the presence of hydrogen peroxide to degrade rifampicin in aqueous media.

Key Words: Pharmaceuticals, Rifampicin, Iron nanoparticles, Catalytic activity, Kinetics

Introduction

Pharmaceutical products have been widely utilized by both humans and animals across the globe (Demirezen, Yıldız, & Yılmaz, 2019; Kansal et al., 2014; Pantelidou et al., 2015; Smýkalová, Sokolová, Foniok, Matejka, & Praus, 2019). This is because of the increase in the morbidity rate and developed resistance of pathogens to the available antimicrobial drugs (Demirezen et al., 2019; Kairigo, Ngumba, Sundberg, Gachanja, & Tuhkanen, 2020). The pronounced use of pharmaceuticals is linked to their ability to diagnose, treat, as well as prevent the occurrence of various diseases thus improving the quality of millions of life (Kansal et al., 2014). However, presence of pharmaceutical compounds in wastewater has been reported to be a global concern as it can affect aquatic habitats and cause increased population of antimicrobial resistance pathogens present in waste water (Kairigo et al., 2020; Kansal et al., 2014). The high prevalence of these drugs in most wastewater bodies has not been established. However, various mechanisms in which these compounds get into water bodies can be linked to the increased population in urban areas, poor housing, improper disposal of waste, improper

drainage, human and animal excretion leading to poor hygiene and confined water treatment methods which are not designed for treatment of waste water with pharmaceuticals at low concentrations (Teixeira et al., 2016). Most of the pharmaceuticals may not be metabolized completely hence, can be excreted in their initial or transformed form through disposals from hospitals and household and human and animal excretion, hence need for development of effective methods of transforming them into nontoxic and biodegradable forms or efficiently remove them from the environment (Kansal et al., 2014; Smýkalová et al., 2019). Various methods have been employed to remove them from wastewater whose efficiency seems to depend on their physical and chemical properties. Activated sludge method and biological treatment have been employed and have not been feasible as they produce toxic chemicals to living organisms (Bhamare & Kulkarni, 2019; Leal, Thompson, & Brzezinski, 2010). Hence, there is need for finding new, effective, and efficient degradation methods for pharmaceuticals and their products in wastewater to transform them to less toxic and more biodegradable forms. The oxidation processes have been reported for the removal of these organic compounds in wastewater. These include membrane filtration, activated carbon adsorption, photolysis, advanced oxidation, ozonation, sonolysis, hydrogen peroxide and heterogeneous photo catalysis (Andreozzi, Canterino, Marotta, & Paxeus, 2005; Andreozzi, Caprio, Marotta, & Radovnikovic, 2003; Das et al., 2018; Doll & Frimmel, 2003; Yargeau & Danylo, 2015). Advanced oxidation method seems to be the best candidate in the elimination of organic pollutants as they mineralize contaminants into carbon dioxide, water, and biodegradable and harmless compounds (dos Santos, Cervantes, & van Lier, 2007; Kansal et al., 2014; Teixeira et al., 2016). Different metal oxide nanoparticles such as titanium, iron, platinum, zinc and zirconium have been employed successfully as semiconductor photo catalysts in the removal of pharmaceuticals through filtration, adsorption, photo catalysis and Fenton methods with hydrogen peroxide as an oxidizing agent which generates hydroxyl radicals which attack and oxidize the organic pollutants (Bhamare & Kulkarni, 2019; W. Cai, Weng, & Chen, 2019; Das et al., 2018; De Andrade, Oliveira, Da Silva, & Vieira, 2018; Demirezen et al., 2019; Kansal et al., 2014; Malakootian, Nasiri, & Amiri Gharaghani, 2020; Mbiri et al., 2018; Teixeira et al., 2016). Barium Doped zinc oxide nanoparticles were used by Bhamare and Kulkarni to photo catalytically degrade Zidovudine an antiretroviral agent for AIDs which was dependent on the amount of the catalyst (Bhamare & Kulkarni, 2019). Titanium oxide nanoparticles have shown the best possibility as a catalyst in degradation of levofloxacin, ciprofloxacin, meloxicam with over 80% percentage degradation within 60 minutes (Kansal et al., 2014; Malakootian et al., 2020; Nadim, Al-Ghobashy, Nebsen, & Shehata, 2015; Nasuhoglu, Rodayan, Berk, &

Yargeau, 2012). Removal of rifampicin from an aqueous solution has been done using recyclable iron oxide nanoparticles through adsorption rather than catalytic method which gave a removal efficiency of 61.5% in about 60 minutes. Metallic nanoparticles can be synthesized using various physical and chemical methods which include milling, sodium borohydride and solvothermal methods which have proved inefficient due to the toxic byproducts that cause undesired environmental effects, and the nanoparticle produced especially iron nanoparticles tents to agglomerate due to the van der Waals and magnetic (H. Cai et al., 2013; Huang, Wang, Hu, Lv, & Li, 2017; Ibrahem et al., 2012; Saif, Tahir, & Chen, 2016). Currently, biological methods using microorganisms and plant extracts are being employed in synthesis of metallic nanoparticles through reduction of metal ions by the sugars, proteins and phenolic metabolites found in the extracts which significantly converts Fe^{3+} ions to iron nanoparticles through bio reduction (Madivoli, Kareru, Gachanja, Mugo, & Sujee, 2019; V. V. Makarov et al., 2014; Valentin V. Makarov et al., 2014; Wanakai et al., 2019). The synthesized iron nanoparticles have been reported to have catalytic property in the degradation of organic dyes and removal of heavy metals in the presence of hydrogen peroxide which initiates the production of radicals and primarily acts as the degradant (Madivoli, Kareru, Gachanja, et al., 2019; Madivoli, Kareru, Maina, et al., 2019; Nyabola, Kareru, Madivoli, Wanakai, & Maina, 2020; Wanakai et al., 2019). In this study, iron oxide nanoparticles were synthesized using leaves from three plants- *Galinnsoga parviflora*, *Conyza bonariensis* and *Bidens pilosa* and their ability to catalytically degrade Rifampicin as a model pollutant was studied at various time, dosage, pH and temperature and the kinetics evaluated using UV–Vis spectrophotometer. The functional groups of the nanoparticles before and after degradation at various conditions were monitored using Fourier Transform infrared spectrophotometer.

Materials and Methods

Collection of Plant Extracts

Fresh leaves of *Galinsoga parviflora, Conyza bonariensis,* and *Bidens pilosa* were collected washed thoroughly with distilled water and air-dried at room temperature (20-25°C) over the laboratory working benches for 14 days to remove moisture and finely ground using a milling machine (Igwe & Nwamezie, 2018).

Preparation of Iron Oxide Nanoparticles

Twenty grams of the ground plant materials were weighed and added to 200 mL of distilled water in different labelled conical flasks, and the mixtures boiled at 75ºC for 30 minutes while shaking. The extracts were filtered through a Whatman no.1 filter paper and stored before use

(Izadiyan et al., 2018; Jeyasundari et al., 2017; Kanagasubbulakshmi & Kadirvelu, 2017; Wanakai et al., 2019). 0.1M $FeCl_3$ was prepared by dissolving 13.5g of $FeCl_3.6H_2O$ in 100 mL of distilled water and topped to 500 mL with distilled water (Fazlzadeh et al., 2017; Nyabola, Kareru, Madivoli, Maina, & Wanakai, 2018). Synthesis of the iron oxide nanoparticles was done by adding the extracts to 0.1M Ferric chloride solution dropwise using a burette in the ratio of 5:1, 4:1, 3:1, 2:1, 2:2, 3:2 respectively with frequent stirring at room temperature and pressure (Balamurugan, Saravanan, & Soga, 2014; Borja et al., 2015; Fazlzadeh et al., 2017; Wanakai et al., 2019). The black precipitate produced was washed several times with distilled water and the obtained nanoparticles were dried at 60°C in the oven. The structure, morphology and composition of the synthesized iron nanoparticles were characterized and are already reported in literature (Wanakai et al., 2019).

Characterization of the Nanoparticles

The synthesized nanoparticles were characterized using UV-Vis, FTIR, SEM, XRD, and XRF as reported by Wanakai *et al*., 2018.

Catalytic Degradation Studies

Degradation of rifampicin using iron oxide nanoparticles was studied using previously established methods with some modifications (Kansal et al., 2014). 0.0025g of rifampicin was dissolved in 1mL of methanol in a 50ml beaker and 10mL of distilled water was added and the contents were transferred into 250mL volumetric flask to make 10 mg/L (12.15 µM). The volumetric flask was topped to the mark by washing the contents in the beaker with distilled water. The degradation experiments were carried out using 12.15 µM rifampicin, 10 mg iron oxide nanoparticles and 250 µL of H_2O_2 solution. The sample was scanned in the range 600-350 nm in 2 min interval using a Shimadzu 1800 UV–Vis spectrophotometer (Shimadzu Corporation, Kyoto, Japan). 250 µL of hydrogen peroxide was added and two spectral scans were taken after which 50 mg of the iron nanoparticles were added into the solution and more scans taken. Separate scans of hydrogen peroxide as a control were taken under the same condition (Bhamare & Kulkarni, 2019). To determine how different reaction parameters affected the rate of degradation of rifampicin, the reactions were carried by varying the adsorbent dose, temperatures, and pH of the reaction media. The degradation was studied at pH 3, 7 and 12 in which the pH of the reaction media was adjusted using 0.1M NaOH and 0.1M HCl. The removal efficiency was calculated using equation 1 where C_0 is the initial concentration and C_t is the rifampicin concentration at time t in minutes (Xu, Owens, & Chen, 2020).

$$Degradation\ efficiency\ (\%) = \frac{C_0 - C_t}{C_0}\ x\ 100 \ldots\ldots\ldots\ldots..(1)$$

The order of the reaction was determined experimentally by plotting the data through assuming a first-order reaction (equation 2) and a second-order reaction (equation 3). The reaction order was determined from the best line of fit obtained from the graph (Atkins & Paula, 2009; Demirezen et al., 2019; Ebbing & Gammon, 2009).

$$ln[A]_t = -kt + \ln[A]_0 \ldots\ldots\ldots.(2)$$

$$\frac{1}{[A]_t} = -kt + \frac{1}{[A]_0} \ldots\ldots\ldots.(3)$$

The thermodynamic parameters associated with rifampicin degradation were determined based on the linear form of van't Hoff equation:

$$\ln K_{eq} = \frac{\Delta H}{RT} + \frac{\Delta S}{R}$$

Where ΔH, and ΔS denote the enthalpy, and entropy of the degradation reaction while R is the universal gas constant and T refers to the temperature (kelvin) (Atkins & Paula, 2009; Ebbing & Gammon, 2009).

Results and Discussions

Variation of the pH of the Reaction Media

The effect of the pH on the catalytic degradation of rifampicin by iron oxide nanoparticles was studied and the results are depicted in figure 1- 5.

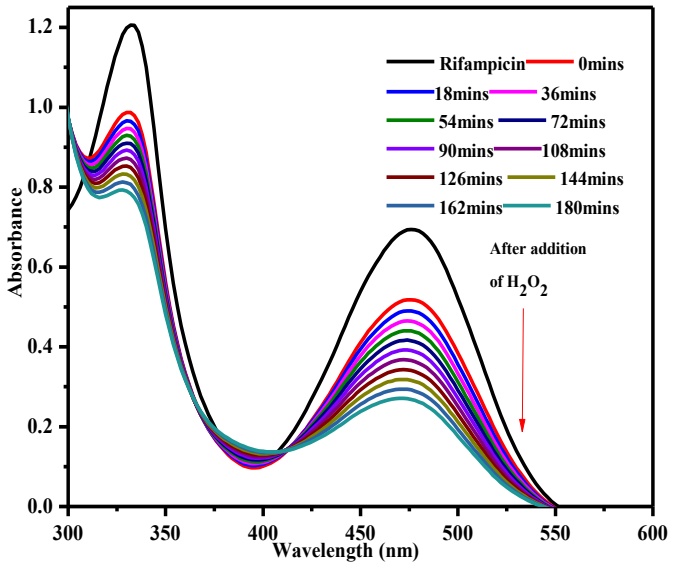

Figure 1: Degradation of Rifampicin in the presence of H_2O_2 at pH 6.5.

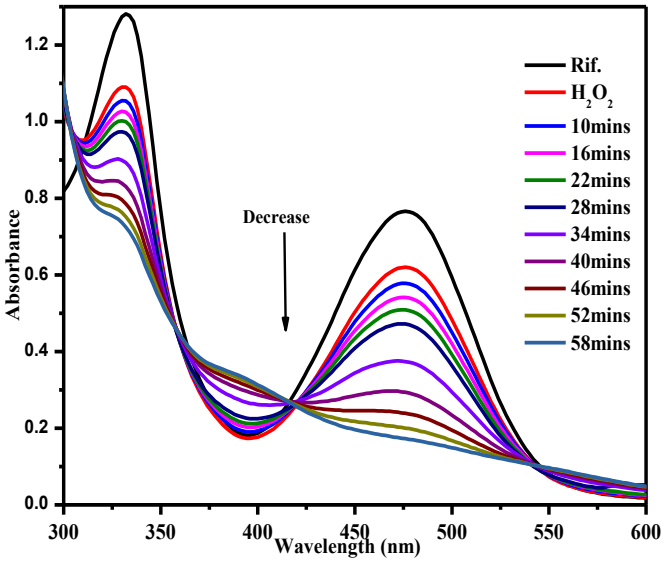

Figure 2: Degradation of Rifampicin (Rif) by CbNPs in the presence of H_2O_2 at pH 6.5

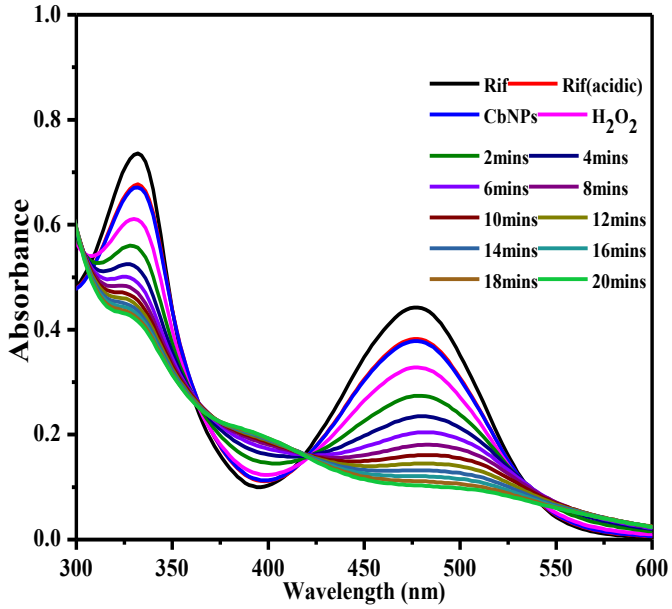

Figure 3: Degradation of Rifampicin (Rif) by CbNPs in the presence of H_2O_2 at pH 3

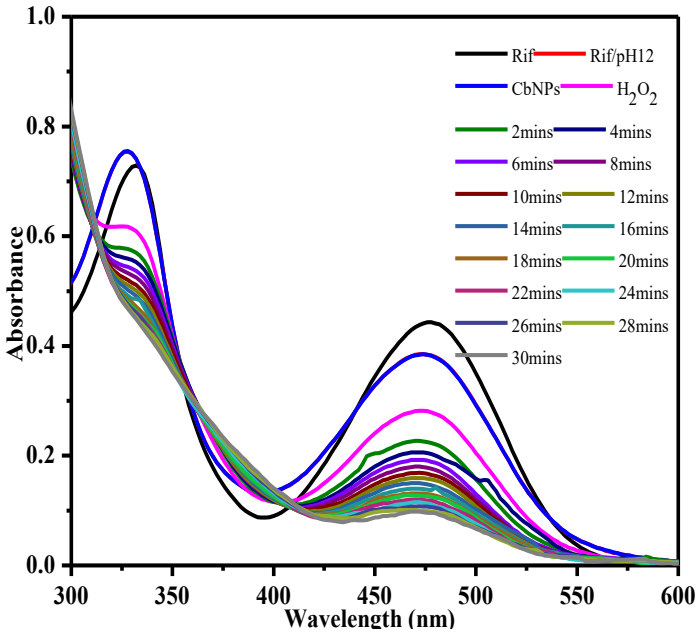

Figure 4: Degradation of Rifampicin (Rif) by CbNPs in the presence of H_2O_2 pH 12

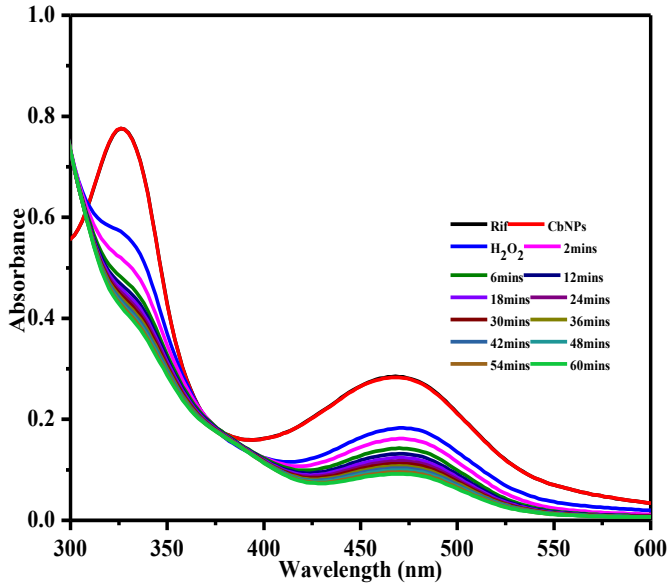

Figure 5: Degradation of Rifampicin (Rif) by CbNPs in the presence of H_2O_2 pH 7

From figure 1-5 (Figure S1-S6), variation of the pH of the reaction media resulted in a remarkable decrease in the absorption intensity of the solution. Upon altering the pH to either acid or basic media, a hypsochromic shift in the absorption intensities of rifampicin attributed to changes in the solution were observed. At pH 3 and 12, the rate of rifampicin degradation was higher as it took approximately between 10 and 30 min for the drug to be degraded confirmed by the rapid decrease in the absorption intensities centered at 480 nm respectively. As it can be observed, the iron nanoparticle synthesized by the three different types of plant extracts had different degradation rates at the pH under study. BpNPs, CbNPs and GpNPs/H_2O_2 at pH 3 degraded rifampicin in 12, 20 and 16 minutes and at pH 12 in 24, 24 and 30 minutes with removal efficiencies of over 80% (figure 3) and (FS 1 - 6). When both hydrogen peroxide and the nanoparticles were used during the degradation experiments, the rate of degradation was observed to be even higher as compared to only the nanoparticle or hydrogen peroxide alone were used. This was attributed to the generation of addition hydroxyl radical when the nanoparticles interacted with hydrogen peroxide hence the observed increase in the rate of degradation (Chauhan, Sillu, & Agnihotri, 2018; Liu, Sutton, Rijnaarts, & Langenhoff, 2016; Pantelidou et al., 2015). Altering the pH of the solution led to a faster rate of degradation in both the basic and acidic environment. The increase in degradation in the basic media is attributed to the increase in the hydroxyl groups which activates the active sites of the nanoparticles thus initiating the reaction. In acidic media, the removal efficiency is higher as the nanoparticles are more positively charged leading to collision with hydrogen peroxide producing numerous hydroxyl radicals (W. Cai et al., 2019; Rezaei & Vione, 2018; Weng, Jin,

Lin, Naidu, & Chen, 2016). The basic environment was not favored as compared to the acidic due to the formation of an oxide layer on the surface of the nanoparticles which decreases the diffusion of rifampicin into the nanoparticles, thereby reducing the production of hydrogen ions and deactivation of the active site (Demirezen et al., 2019; Rezaei & Vione, 2018).

Variation of FeNPs Dose on degradation of Rifampicin

The effect of the amount of iron oxide nanoparticles on the rate of the degradation was studied and the results are depicted in figure 7.

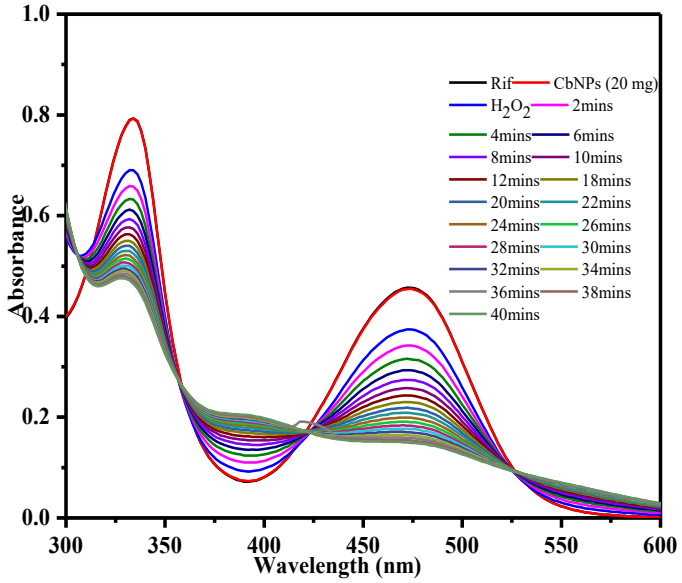

Figure 7: Degradation of Rifampicin (Rif) by 20 mg of CbNPs in the presence of H_2O_2

From figure 7 (Figure S7-S9), increase in the catalyst dose to 20 mg increased the rate at which rifampicin was degrade as compared to when the amount of catalyst used was 1 mg. It was observed that when the amount of iron oxide nanoparticles used was 20 mg, the percent degradation achieved, and the time required to degrade the antibiotic were 65% and 45 min, respectively. It was observed that as the dose increased, the rate of removal also increased due to the increase in the total surface area to volume ratio of the nanoparticles, which increased the high pore- filling effect and active sites needed for producing the radicals needed to degrade the antibiotic (W. Cai et al., 2019; Chauhan et al., 2018; Nasuhoglu et al., 2012; Rezaei & Vione, 2018; Teixeira et al., 2016; Weng et al., 2016).

Variation of Reaction Temperature

The effect of the reaction temperature on the rate of degradation was evaluated and the results are depicted in figure 8 – 11.

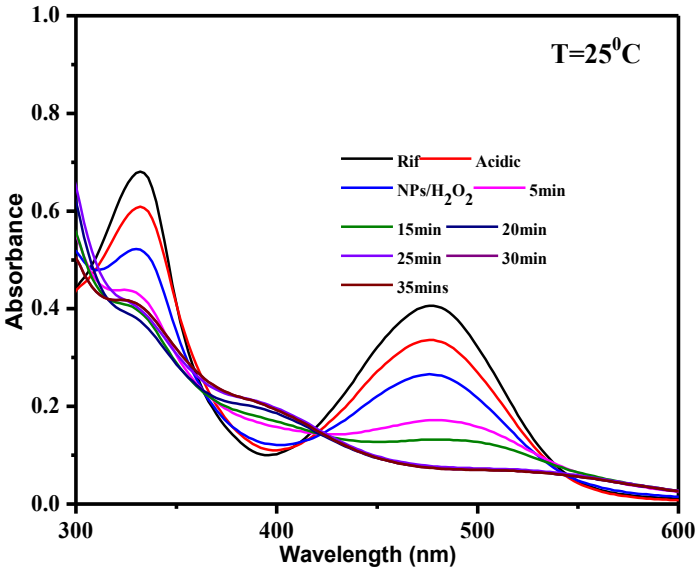

Figure 8: Degradation of rifampicin using iron oxide nanoparticles at 25 ℃

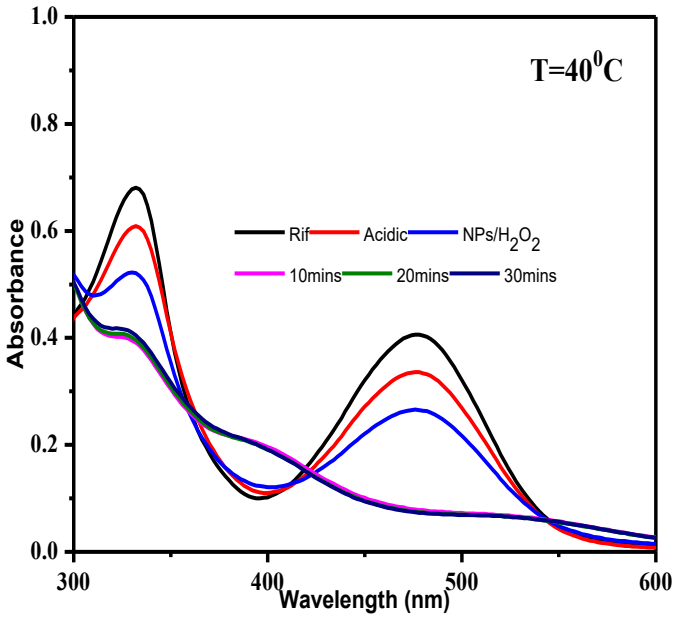

Figure 9: Degradation of rifampicin using iron oxide nanoparticles at 40 ℃

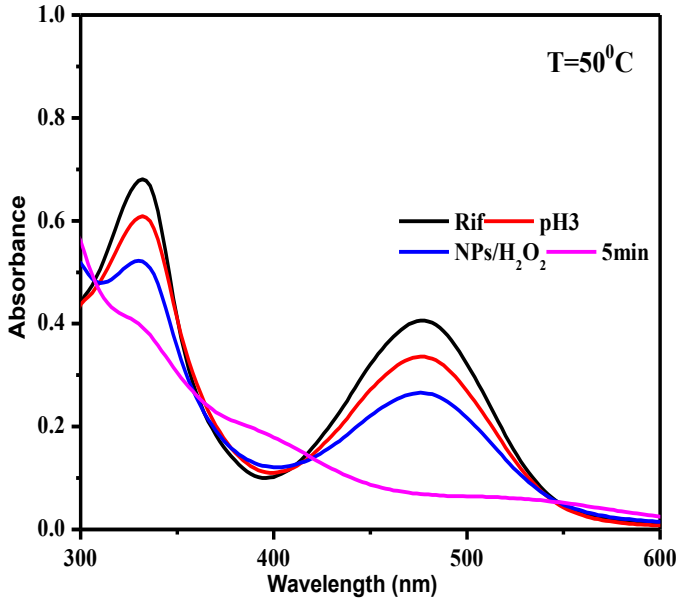

Figure 10: Degradation of rifampicin using iron oxide nanoparticles at 50 ℃

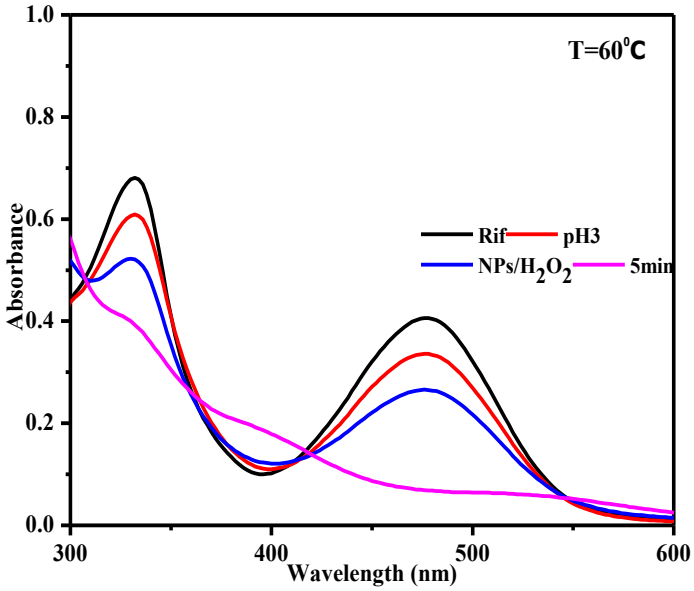

Figure 11: Degradation of rifampicin using iron oxide nanoparticles at 60 ℃

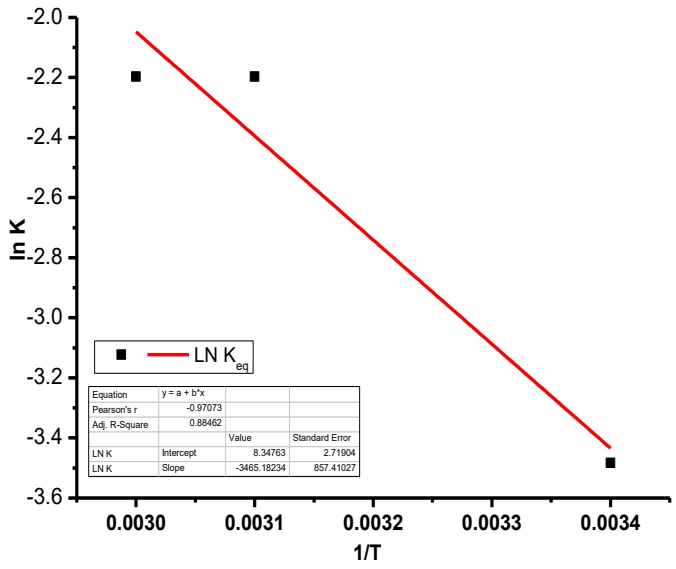

Figure 12: Van't Hoff plot of degradation of rifampicin obtained by plotting ln K_{eq} against 1/T

From figure 8 – 11 (Figure S10-S12), it was observed that the degradation of rifampicin was temperature dependent as at higher temperature it took 5 minutes for the antibiotic to be degraded unlike at lower temperature. Initially, upon addition of HCl into the reaction vessel, a hypsochromic shift was observed in the spectra which can be attributed to a change in the solution pH. For this type of reaction, Le Chatelier's principle predicts that if the temperature increases, the system must shift to the left to alleviate the stress of additional heat. A shift to the left leads to a decrease in products and an increase in reactants, which decreases the equilibrium constant as predicted by the van't Hoff equation (Atkins & Paula, 2009). The degradation of rifampicin (figure 12) was an endothermic reaction which implies that at higher temperatures the rate of degradation was higher. For an endothermic reaction, there is an increase in entropy of the reaction which is reduced when the temperature of the reaction system is raised and the reaction moves towards formation of the products, in this case degradation of rifampicin. The temperature dependence of the equilibrium constant provided a basis in which ΔH and ΔS were experimentally determined from the slope and intercept of the curve in this case 28.81 kJ $mol^{-1}$and 69.39 J mol^{-1} respectively (Atkins & Paula, 2009).

Degradation Efficiency under Different Conditions

The degradation efficiency of iron oxide nanoparticles was evaluated under different reaction conditions and the results are depicted in table 1 and figure 13.

Table 1: Percentage degradation efficiency of rifampicin under various reaction conditions

Reaction Parameters	% degradation	Time (min)
H_2O_2	--	180
CbNPs/ H_2O_2/pH 7	67.98	68
CbNPs/ H_2O_2/pH 6.5	78.12	58
CbNPs/ H_2O_2/ pH 3	86.80	20
CbNPs/ H_2O_2/ pH 12	87.73	30

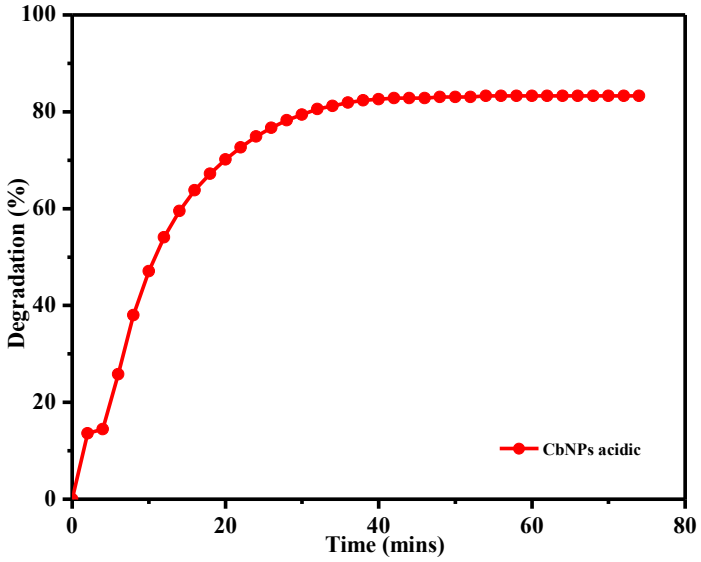

Figure 13: Percent degradation of Rifampicin using iron oxide nanoparticles synthesized using CB

From figure 13, a plot of percent degradation against time revealed that the amount of rifampicin degraded increase when the reaction time was subsequently increased, and it remained constant after 40 minutes. This can be attributed to increased reaction time, resulting in increased interaction between the generated hydroxyl radicals which subsequently increased in the amount of rifampicin decomposed (Madivoli, Kareru, Maina, et al., 2019; Wanakai et al., 2019). The linearity of the graph observed at the end of the reaction can be attributed to a decrease in the number of radical generated and a decrease in the concentration of the antibiotic towards the end of the reaction. This correlates with a significant decrease in the absorption intensity observed indicating a considerable decrease in the concentration of rifampicin in the presence of the iron nanoparticles and hydrogen peroxide (Kansal et al., 2014; Madivoli, Kareru, Maina, et al., 2019). The percent degradation of rifampicin was found to be between 75-80% when hydrogen peroxide was used together with iron nanoparticles synthesized by the three extracts.

FTIR Analysis

The infrared spectra of iron oxide nanoparticles before and after degradation under different reaction conditions are depicted in figures 14.

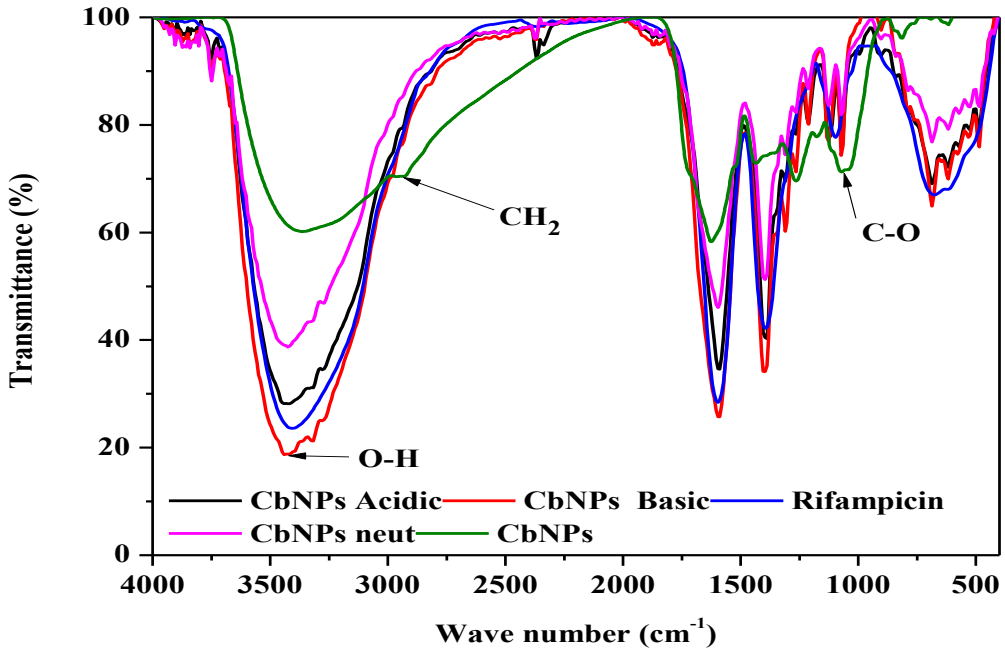

Figure 14: FTIR Spectra of Rifampicin and *C. bonariensis* iron oxide nanoparticles before and after degradation in acidic pH

The FTIR spectra of the synthesized iron oxide nanoparticles were reported by (Wanakai et al., 2019) where the O-H stretching vibration was present in CbNPs, BpNPs and GpNPs at 3406 cm^{-1}, 3402.6 cm^{-1} and 3438.3 cm^{-1} while the C–O-C glycosidic linkages at 1027 cm^{-1}, 1031 cm^{-1} and 1037.7 cm^{-1} and the C=C was reported as a vibrational mode for the unsaturated metabolites which were depicted by the vibrational bands at 1630, 1631 and 1627.4 cm^{-1} in , CbNPs, BpNPS and GpNPs respectively. From the spectra obtained, rifampicin shows the organic nature by the numerous peaks of carbon, nitrogen, and oxygen in the range of 800-1200cm^{-1}. Rifampicin showed a broad band at 3419cm^{-1} which was due to the O-H bending vibrations (W. Cai et al., 2019). It was observed that the FTIR spectra of the nanoparticles before and after exposure to rifampicin showed relatively a number of changes in various peaks indicating that the nanoparticles were relatively stable but had acquired the characteristic properties of rifampicin through adsorption FS 29 and 30 (Xu et al., 2020). There was addition of the number of peaks of the nanoparticles after degradation at 1121 cm^{-1} with slight shifts of

the peaks. The peak at 1630 cm^{-1} in the nanoparticles shifted to 1602 cm^{-1} while those at 1255cm^{-1} shifted to 1393 cm^{-1}. In addition, the sizes of the peaks of the nanoparticles after degradation had increased in the intensity. This is attributed to the adsorption of the rifampicin on to the surface of the iron oxide nanoparticles which increases the number of the functional groups (W. Cai et al., 2019; Xu et al., 2020).

Degradation Kinetics of Rifampicin

The pseudo first order and second order were used to analyze the kinetics of the catalytic removal of rifampicin at various conditions by iron oxide nanoparticles and the results are depicted in figures 15 – 19, (FS 13 – 29) and table 2.

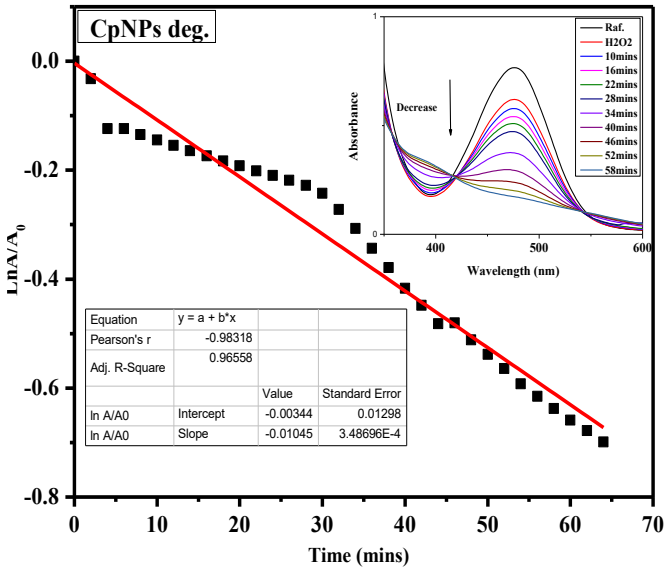

Figure 15: First order plot of rifampicin degradation using CbNPs/H_2O_2. Insert time dependent UV–Vis absorption spectra

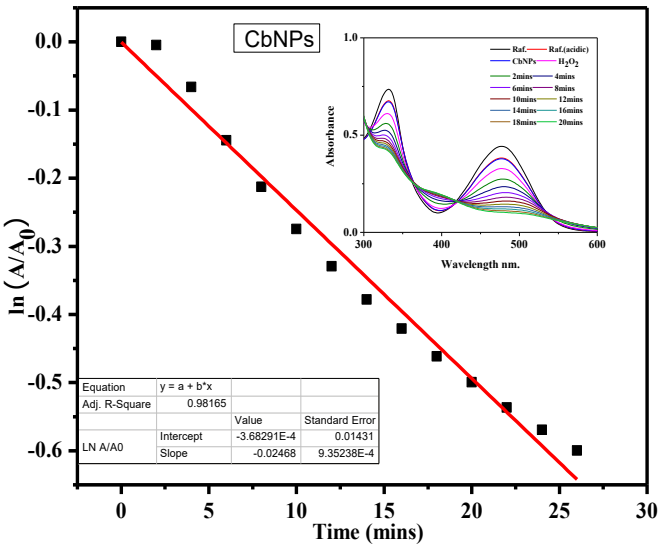

Figure 16: First order plot of rifampicin degradation using CbNPs/H_2O_2 at pH 3. Insert time dependent UV–Vis absorption spectra

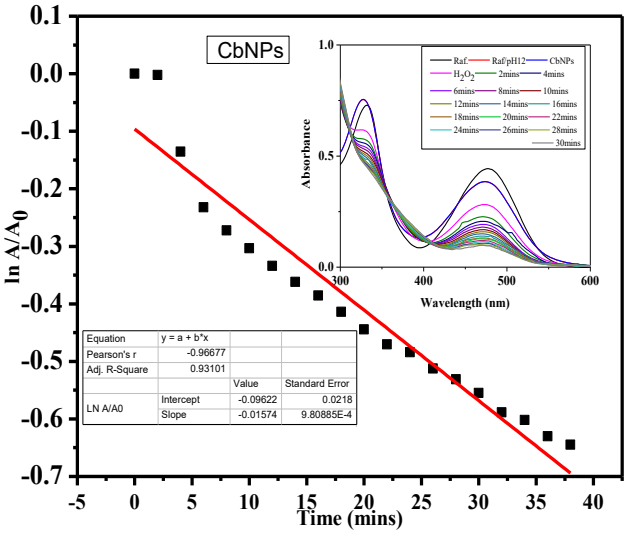

Figure 17: First order plot of rifampicin degradation using CbNPs/H_2O_2 at pH 12. Insert time dependent UV–Vis absorption spectra

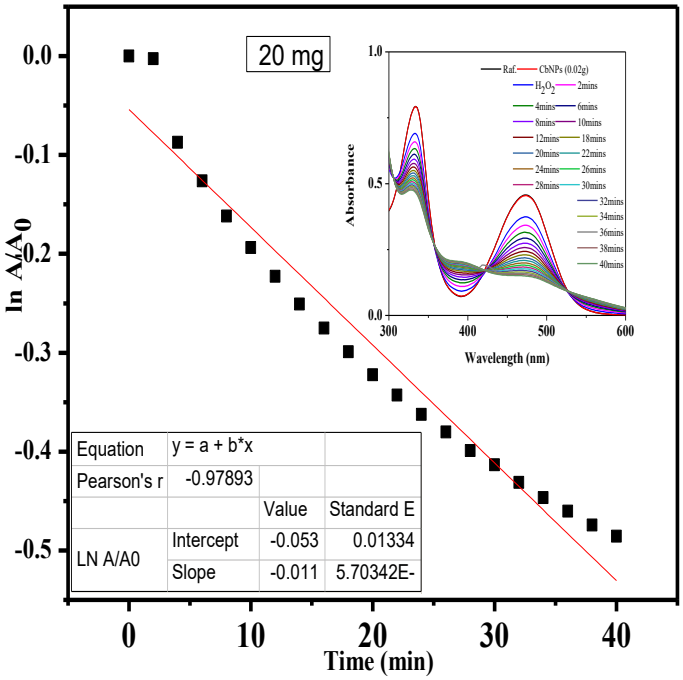

Figure 18: First order plot of rifampicin degradation using 20 mg of CbNPs. Insert time dependent UV–Vis absorption spectra

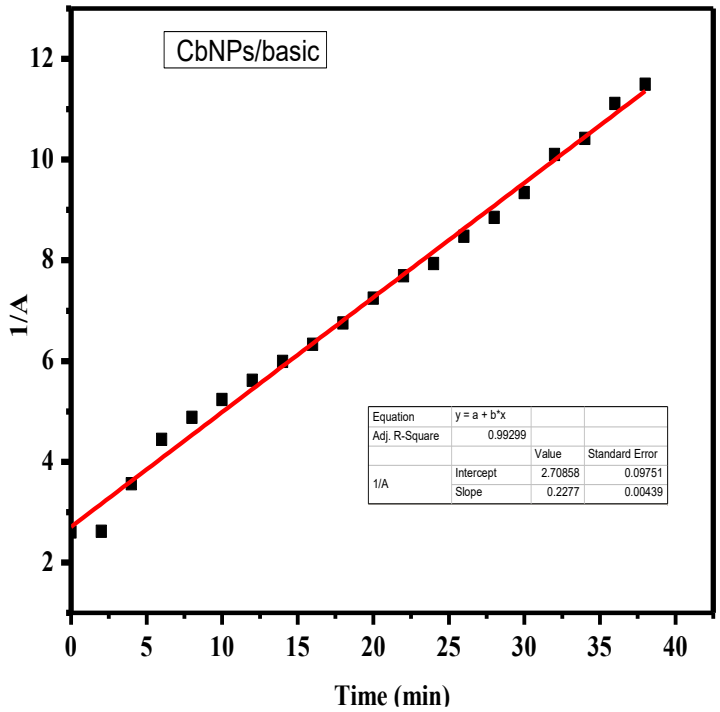

Figure 19: Second order kinetics for the degradation of rifampicin by CbNPs/H_2O_2 at pH 12

Table 2: Rate constant (k) for degradation of rifampicin at different pH and dosage

Sample ID	pH	1st Order		2nd Order		Rate (µmol/L min)
		R^2	k	R^2	k	
BpNPs	3	0.9408	-0.0420	0.9004	0.5390	-2.1×10^{-2}
CbNPs	3	0.9817	-0.0247	0.8022	0.1547	-3.0×10^{-3}
GpNPs	3	0.9917	-0.0029	0.9829	0.3548	-1.4×10^{-2}
BpNPs	12	0.9339	-0.0131	0.9764	0.1267	-7.8×10^{-3}
CbNPs	12	0.9310	-0.0167	0.9930	0.2277	-6.6×10^{-3}
GpNPs	12	0.9709	-0.0200	0.9902	0.2178	-1.1×10^{-2}
BpNPs	7	0.8211	-0.0127	0.9334	0.1024	-3.2×10^{-3}
CbNPs	7	0.7914	-0.0084	0.9122	0.1409	-2.9×10^{-3}
GpNPs	7	0.9167	-0.0117	0.9685	0.1130	-7.2×10^{-3}
20mg	7	0.9688	-0.0200	0.9969	0.1150	-7.1×10^{-3}
10mg	7	0.9561	-0.0119	0.9008	0.0310	-3.5×10^{-3}
5mg	7	0.9389	-0.0045	0.8593	0.0196	-3.3×10^{-3}
1mg	7	0.8894	-0.0027	0.4333	0.0579	-2.1×10^{-3}
25 ℃		0.9122	-0.0307	0.9297	0.2242	-8.9×10^{-3}
40 ℃		0.8983	-0.0124	0.8837	0.4621	-1.2×10^{-2}
50 ℃		0.8924	-0-1112	0.8292	0.7505	-2.4×10^{-2}
60 ℃		0.8924	-0.1112	0.8292	0.7505	-7.7×10^{-2}

The rate constants for the degradation of rifampicin at various reaction conditions are listed in table 2. Depending on pH and dosage, the kinetic data revealed that the degradation of rifampicin followed a pseudo second order model rather than a first order model because most of the R^2 values in second order were higher, which showed that the degradation process is pH dependent as the protons play an important role in the generation of the hydroxyl groups (W. Cai et al., 2019). In addition, the acidic pH alters the superficial charge of the nanoparticles improving their degree of ionization and electrostatic interactions with the organic molecule thereby destroying it (Malakootian et al., 2020). The faster rate of degradation is also attributed to the ability of the protons to destroy the iron complexes and precipitants which helps recovery of fresh and active sites (Velichkova, Julcour-Lebigue, Koumanova, & Delmas, 2013).

Conclusion

The present study reports green synthesis of iron oxide nanoparticles using *Galinsoga parviflora, Conyza bonariensis* and *Bidens pilosa leaf extracts* in a simple, costly effective, and ecofriendly method. The nanoparticles were found to have catalytic property as they efficiently degraded rifampicin an emerging pollutant that is commonly found in contaminated water and is hard to remove. The influence of pH, dosage, temperature and concentration on the rate of degradation were evaluated and found to have an impact on the rate of removal. The

kinetics of degradation were evaluated by fitting the experimental data to first order and second order kinetics while thermodynamic parameters were evaluated by fitting the experimental data to Van't Hoff's equation. The degradation of rifampicin was found to follow second order kinetics as compared to first order kinetics and the reactions were endothermic with rate of degradation greatly enhance at higher temperature. Hence iron oxide nanoparticles synthesized using the three plant extracts could be used as a catalyst to enhance the degradation of the antibiotic which is an emerging pollutant.

Acknowledgement:

The authors would like to acknowledge the Chemistry Department Jomo Kenyatta University of Agriculture and Technology for providing necessary laboratory facilities.

Conflict of interest: The authors declare that they do not have conflict of interest.

References

Andreozzi, R., Canterino, M., Marotta, R., & Paxeus, N. (2005). Antibiotic removal from wastewaters: The ozonation of amoxicillin. *Journal of Hazardous Materials*, *122*(3), 243–250. https://doi.org/10.1016/j.jhazmat.2005.03.004

Andreozzi, R., Caprio, V., Marotta, R., & Radovnikovic, A. (2003). Ozonation and H2O2/UV treatment of clofibric acid in water: A kinetic investigation. *Journal of Hazardous Materials*, *103*(3), 233–246. https://doi.org/10.1016/j.jhazmat.2003.07.001

Atkins, P., & Paula, J. De. (2009). Atkins' Physical chemistry 8th edition. *Chemistry*, pp. 430–468. https://doi.org/10.1021/ed056pA260.1

Balamurugan, M., Saravanan, S., & Soga, T. (2014). Synthesis of Iron Oxide Nanoparticles by Using Eucalyptus Globulus Plant Extract. *E-Journal of Surface Science and Nanotechnology*, *12*(0), 363–367. https://doi.org/10.1380/ejssnt.2014.363

Bhamare, V. S., & Kulkarni, R. M. (2019). Photocatalytic degradation of pharmaceutical drug zidovudine by undoped and 5 % barium doped zinc oxide nanoparticles during water treatment: Synthesis and characterisation. *International Journal of Applied Pharmaceutics*, *11*(1), 227–236. https://doi.org/10.22159/ijap.2019v11i1.30350

Borja, J. Q., Ngo, M. A. S., Saranglao, C. C., Tiongco, R. P. M., Roque, E. C., & Dugos, N. P. (2015). Synthesis of green zero-valent iron using polyphenols from dried green tea extract. *Journal of Engineering Science and Technology*, *10*(Spec.issue7), 22–31.

Cai, H., An, X., Cui, J., Li, J., Wen, S., Li, K., … Shi, X. (2013). Facile hydrothermal synthesis and surface functionalization of polyethyleneimine-coated iron oxide nanoparticles for

biomedical applications. *ACS Applied Materials and Interfaces*, *5*(5), 1722–1731. https://doi.org/10.1021/am302883m

Cai, W., Weng, X., & Chen, Z. (2019). Highly efficient removal of antibiotic rifampicin from aqueous solution using green synthesis of recyclable nano-Fe3O4. *Environmental Pollution*, *247*, 839–846. https://doi.org/10.1016/j.envpol.2019.01.108

Chauhan, A., Sillu, D., & Agnihotri, S. (2018). Removal of Pharmaceutical Contaminants in Wastewater Using Nanomaterials: A Comprehensive Review. *Current Drug Metabolism*, *20*(6), 483–505. https://doi.org/10.2174/1389200220666181127104812

Das, S., Ghosh, S., Misra, A. J., Tamhankar, A. J., Mishra, A., Lundborg, C. S., & Tripathy, S. K. (2018). Sunlight assisted photocatalytic degradation of ciprofloxacin in water using fe doped zno nanoparticles for potential public health applications. *International Journal of Environmental Research and Public Health*, *15*(11), 1–11. https://doi.org/10.3390/ijerph15112440

De Andrade, J. R., Oliveira, M. F., Da Silva, M. G. C., & Vieira, M. G. A. (2018). Adsorption of Pharmaceuticals from Water and Wastewater Using Nonconventional Low-Cost Materials: A Review. *Industrial and Engineering Chemistry Research*, *57*(9), 3103–3127. https://doi.org/10.1021/acs.iecr.7b05137

Demirezen, D. A., Yıldız, Y. Ş., & Yılmaz, D. D. (2019). Amoxicillin degradation using green synthesized iron oxide nanoparticles: Kinetics and mechanism analysis. *Environmental Nanotechnology, Monitoring and Management*, *11*, 100219. https://doi.org/10.1016/j.enmm.2019.100219

Doll, T. E., & Frimmel, F. H. (2003). Fate of pharmaceuticals - Photodegradation by simulated solar UV-light. *Chemosphere*, *52*(10), 1757–1769. https://doi.org/10.1016/S0045-6535(03)00446-6

dos Santos, A. B., Cervantes, F. J., & van Lier, J. B. (2007). Review paper on current technologies for decolourisation of textile wastewaters: Perspectives for anaerobic biotechnology. *Bioresource Technology*, *98*(12), 2369–2385. https://doi.org/10.1016/j.biortech.2006.11.013

Ebbing, D. D., & Gammon, S. D. (2009). *General chemistry* (11th ed.). Boston: Houghton Mifflin Company.

Fazlzadeh, M., Rahmani, K., Zarei, A., Abdoallahzadeh, H., Nasiri, F., & Khosravi, R. (2017). A novel green synthesis of zero valent iron nanoparticles (NZVI) using three plant extracts and their efficient application for removal of Cr(VI) from aqueous solutions. *Advanced Powder Technology*, *28*(1), 122–130. https://doi.org/10.1016/j.apt.2016.09.003

Huang, G., Wang, M., Hu, Y., Lv, S., & Li, C. (2017). Synthesis, characterization, and debromination reactivity of cellulosestabilized Pd/Fe nanoparticles for 2,2',4,4'-tretrabromodiphenyl ether. *PLoS ONE*, *12*(3), 1–17. https://doi.org/10.1371/journal.pone.0174589

Ibrahem, A. K., Abdel Moghny, T., Mustafa, Y. M., Maysour, N. E., Mohamed Saad El Din El Dars, F., & Farouk Hassan, R. (2012). Degradation of Trichloroethylene Contaminated Soil by Zero-Valent Iron Nanoparticles. *ISRN Soil Science*, *2012*, 1–9. https://doi.org/10.5402/2012/270830

Igwe, O. U., & Nwamezie, F. (2018). *Green synthesis of iron nanoparticles using flower extract of Piliostigma thonningii and their antibacterial activity evaluation*. (January), 60–66.

Izadiyan, Z., Shameli, K., Miyake, M., Hara, H., Mohamad, S. E. B., Kalantari, K., … Rasouli, E. (2018). Cytotoxicity assay of plant-mediated synthesized iron oxide nanoparticles using Juglans regia green husk extract. *Arabian Journal of Chemistry*. https://doi.org/10.1016/j.arabjc.2018.02.019

Jeyasundari, J., Praba, P. S., Jacob, Y. B. A., Vasantha, V. S., & Shanmugaiah, V. (2017). Green Synthesis and Characterization of Zero Valent Iron Nanoparticles from the Leaf Extract of Psidium Guajava Plant and Their Antibacterial Activity. *Chemical Science Review and Letters*, *6*(22), 1244–1252.

Kairigo, P., Ngumba, E., Sundberg, L. R., Gachanja, A., & Tuhkanen, T. (2020). Occurrence of antibiotics and risk of antibiotic resistance evolution in selected Kenyan wastewaters, surface waters and sediments. *Science of the Total Environment*. https://doi.org/10.1016/j.scitotenv.2020.137580

Kanagasubbulakshmi, S., & Kadirvelu, K. (2017). Green Synthesis of Iron Oxide Nanoparticles using Lagenaria Siceraria and Evaluation of its Antimicrobial Activity. *Defence Life Science Journal*, *2*(4), 422–427.

Kansal, S. K., Kundu, P., Sood, S., Lamba, R., Umar, A., & Mehta, S. K. (2014). Photocatalytic degradation of the antibiotic levofloxacin using highly crystalline TiO2 nanoparticles. *New Journal of Chemistry*, *38*(7), 3220–3226. https://doi.org/10.1039/c3nj01619f

Leal, J. E., Thompson, A. N., & Brzezinski, W. A. (2010). Pharmaceuticals in drinking water: Local analysis of the problem and finding a solution through awareness. *Journal of the American Pharmacists Association*, *50*(5), 600–603. https://doi.org/10.1331/JAPhA.2010.09186

Liu, W., Sutton, N. B., Rijnaarts, H. H. M., & Langenhoff, A. A. M. (2016). Pharmaceutical

removal from water with iron- or manganese-based technologies: A review. *Critical Reviews in Environmental Science and Technology*, *46*(19–20), 1584–1621. https://doi.org/10.1080/10643389.2016.1251236

Madivoli, E. S., Kareru, P. G., Gachanja, A. N., Mugo, S. M., & Sujee, D. M. (2019). Phytofabrication of iron nanoparticles and their catalytic activity. *SN Applied Sciences*, *1*(8), 1–9. https://doi.org/10.1007/s42452-019-0951-0

Madivoli, E. S., Kareru, P. G., Maina, E. G., Nyabola, A. O., Wanakai, S. I., Nyang'au, J. O., & Nyanga'u, J. O. (2019). Biosynthesis of iron nanoparticles using Ageratum conyzoides extracts , their antimicrobial and photocatalytic activity. *SN Applied Sciences*, *1*(5), 1–9. https://doi.org/10.1007/s42452-019-0511-7

Makarov, V. V., Love, A. J., Sinitsyna, O. V., Makarova, S. S., Yaminsky, I. V., Taliansky, M. E., & Kalinina, N. O. (2014). "Green" nanotechnologies: Synthesis of metal nanoparticles using plants. *Acta Naturae*, *6*(20), 35–44. https://doi.org/10.1039/c1gc15386b

Makarov, Valentin V., Makarova, S. S., Love, A. J., Sinitsyna, O. V., Dudnik, A. O., Yaminsky, I. V., … Kalinina, N. O. (2014). Biosynthesis of Stable Iron Oxide Nanoparticles in Aqueous Extracts of *Hordeum vulgare* and *Rumex acetosa* Plants. *Langmuir*, *30*(20), 5982–5988. https://doi.org/10.1021/la5011924

Malakootian, M., Nasiri, A., & Amiri Gharaghani, M. (2020). Photocatalytic degradation of ciprofloxacin antibiotic by TiO2 nanoparticles immobilized on a glass plate. *Chemical Engineering Communications*, *207*(1), 56–72. https://doi.org/10.1080/00986445.2019.1573168

Mbiri, A., Wittstock, G., Taffa, D. H., Gatebe, E., Baya, J., & Wark, M. (2018). Photocatalytic degradation of the herbicide chloridazon on mesoporous titania/zirconia nanopowders. *Environmental Science and Pollution Research*, *25*(35), 34873–34883. https://doi.org/10.1007/s11356-017-1023-x

Nadim, A. H., Al-Ghobashy, M. A., Nebsen, M., & Shehata, M. A. (2015). Optimization of photocatalytic degradation of meloxicam using titanium dioxide nanoparticles: application to pharmaceutical wastewater analysis, treatment, and cleaning validation. *Environmental Science and Pollution Research*, *22*(20), 15516–15525. https://doi.org/10.1007/s11356-015-4713-2

Nasuhoglu, D., Rodayan, A., Berk, D., & Yargeau, V. (2012). Removal of the antibiotic levofloxacin (LEVO) in water by ozonation and TiO 2 photocatalysis. *Chemical Engineering Journal*, *189–190*, 41–48. https://doi.org/10.1016/j.cej.2012.02.016

Nyabola, A. O., Kareru, P. G., Madivoli, E. S., Maina, E. G., & Wanakai, I. S. (2018).

Assessment of the Anti-microbial Action of Zero Valent Iron Nanoparticle Synthesized by Aspilia pluriseta Extracts. *Chemical Science International Journal*, *25*(3), 1–10. https://doi.org/10.9734/csji/2018/45799

Nyabola, A. O., Kareru, P. G., Madivoli, E. S., Wanakai, S. I., & Maina, E. G. (2020). Formation of Silver Nanoparticles via Aspilia pluriseta Extracts Their Antimicrobial and Catalytic Activity. *Journal of Inorganic and Organometallic Polymers and Materials*, (0123456789). https://doi.org/10.1007/s10904-020-01497-7

Pantelidou, N. A., Theologides, C. P., Olympiou, G. G., Savva, P. G., Vasquez, M. I., & Costa, C. N. (2015). Catalytic removal of pharmaceutical compounds in water medium under an H2 stream over various metal-supported catalysts: A promising process. *Desalination and Water Treatment*, *53*(12), 3363–3370. https://doi.org/10.1080/19443994.2014.933620

Rezaei, F., & Vione, D. (2018). Effect of pH on zero valent iron performance in heterogeneous Fenton and Fenton-like processes: A review. *Molecules*, *23*(12). https://doi.org/10.3390/molecules23123127

Saif, S., Tahir, A., & Chen, Y. (2016). Green Synthesis of Iron Nanoparticles and Their Environmental Applications and Implications. *Nanomaterials*, *6*(11). https://doi.org/10.3390/nano6110209

Smýkalová, A., Sokolová, B., Foniok, K., Matejka, V., & Praus, P. (2019). Photocatalytic degradation of selected pharmaceuticals using g-C3N4 and TiO2 nanomaterials. *Nanomaterials*, *9*(9). https://doi.org/10.3390/nano9091194

Teixeira, S., Gurke, R., Eckert, H., Kühn, K., Fauler, J., & Cuniberti, G. (2016). Photocatalytic degradation of pharmaceuticals present in conventional treated wastewater by nanoparticle suspensions. *Journal of Environmental Chemical Engineering*, *4*(1), 287–292. https://doi.org/10.1016/j.jece.2015.10.045

Velichkova, F., Julcour-Lebigue, C., Koumanova, B., & Delmas, H. (2013). Heterogeneous Fenton oxidation of paracetamol using iron oxide (nano)particles. *Journal of Environmental Chemical Engineering*, *1*(4), 1214–1222. https://doi.org/10.1016/j.jece.2013.09.011

Wanakai, S. I., Kareru, P. G., Makhanu, D. S., Madivoli, E. S., Maina, E. G., & Nyabola, A. O. (2019). Catalytic degradation of methylene blue by iron nanoparticles synthesized using Galinsoga parviflora, Conyza bonariensis and Bidens pilosa leaf extracts. *SN Applied Sciences*, *1*(10). https://doi.org/10.1007/s42452-019-1203-z

Weng, X., Jin, X., Lin, J., Naidu, R., & Chen, Z. (2016). Removal of mixed contaminants Cr(VI) and Cu(II) by green synthesized iron based nanoparticles. *Ecological Engineering*,

97, 32–39. https://doi.org/10.1016/j.ecoleng.2016.08.003

Xu, Q., Owens, G., & Chen, Z. (2020). Adsorption and catalytic reduction of rifampicin in wastewaters using hybrid rGO@Fe/Pd nanoparticles. *Journal of Cleaner Production*, *264*, 121617. https://doi.org/10.1016/j.jclepro.2020.121617

Yargeau, V., & Danylo, F. (2015). Removal and transformation products of ibuprofen obtained during ozone- and ultrasound-based oxidative treatment. *Water Science and Technology*, *72*(3), 491–500. https://doi.org/10.2166/wst.2015.234